

# A Multichannel Photon Counting System for Gas Analysis with Raman-Scattering Technique

Panagiotis G. Papageorgas, Harald Winter, Hansjörg Albrecht, Dimitris Maroulis, and Nikiforos G. Theofanous

**Abstract**—A microcontroller-based photon counting system has been developed by the Laser and Medicine-Technology gGmbH, Berlin, Germany, in cooperation with the University of Athens. This microcontroller-based system controls, acquires, processes and stores the data from a high-resolution multichannel gas analyzer based on linear vibrational Raman scattering. The system described provides accurate photon-counting measurements using suitable photomultiplier tubes (PMT's) as detectors of the Raman signals. The implemented system amplifies, discriminates and counts the PMT pulses with a pulse-pair resolution of 5 ns. The specific implementation offers a number of important features such as portability, low power consumption, low cost, increased reliability, high sensitivity, and upgradability, and supports autocalibration and drift-compensation. Moreover, the described photon-counting system can be easily adapted to a broad field of applications, some of which are in the fields of medical electronics (confocal microscopy) and bio-electronics, air pollution measurements with Raman spectrometers, mass spectrometers, laser sounding of the atmosphere, and electro-optical systems, where photomultiplier tubes are typically used in the pulse-counting mode of operation.

**Index Terms**—Air pollution, laser gas sensor, multichannel gas monitoring, optoelectronic measurement system, photon-counting, Raman scattering, Raman spectroscopy.

## I. INTRODUCTION

**R**AMAN spectroscopy of gases has been extensively used in research laboratory, [1]–[3], [5] especially since the development of appropriate laser light sources. The corresponding development of portable multichannel Raman spectrometers has been extremely difficult due mainly to the size of the laser light source and the electronics necessary for the detection and processing of the signals. The recent development of diode-pumped solid state microlasers in the green (532 nm) and blue (457 nm) region of the spectra with adequate power (50–100 mW) and the evolution in the electronics and computer fields has opened the way to the development of portable multichannel systems using the Raman scattering technique.

The described apparatus realizes a multichannel photon-counting system for the *in situ* quantitative monitoring of up to five air pollutants simultaneously and one calibration channel (nitrogen). The electronics of the system comprises six photon-counting modules, one for each channel, and a microcontroller

based processing unit. In the literature, detailed electronic schematics are seldom provided for the realization of a photon-counting system, excepting some few examples [6]–[10]. We will focus for this reason with detail on the electronics and signal handling unit used for the realization of the photon-counting modules and shall also give preliminary results for the entire system operation. First, we will give a short description of the entire system followed by a detailed description of the photon-counting modules, the microcontroller unit and the sensors and actuators necessary for the operation of the system. Performance measurements of the photon-counting module compared with a commercial system are presented together with indicative measurements of sensitivity for gases concentrations.

## II. SHORT DESCRIPTION OF THE ENTIRE MULTICHANNEL RAMAN GAS SENSOR

The multichannel photon-counting system under presentation is the electronic and signal handling part of a complete multichannel Raman gas sensor (MRGS) developed within the framework of a project of European Commission concerning air pollution monitoring. The optical part of this set-up consists of a laser source that excites the mixture of gases under test housed in an appropriate multipass optical resonator, which has the form of a mirror-faced cylinder (cuvette). In Fig. 1, we present a block diagram of the whole system.

The laser sources used were a green and a blue laser. The green laser is a small diode-pumped Nd:YAG solid state laser, where neodymium is a doped rod made of yttrium–aluminum–garnet as the active medium and transposed by SHG to the green (532 nm) spectrum with a power of 100 mW. The blue laser is a Nd:AlV<sub>2</sub>O<sub>7</sub> solid state laser, where neodymium is doped rod, made of aluminum–vanadium oxide as the active medium and transposed by SHG to the blue spectrum (457 nm) with a power of 100 mW. Both lasers are manufactured from Laser Power Co. The laser light excites Raman effect in the (up to six) gases within the cuvette and the corresponding Stokes-shifted Raman scattered light is partitioned, by means of appropriate interference filters, into six spectral channels. The scattered light is received by six corresponding photomultiplier tubes (PMT's) which are arranged in the equatorial plane of the cuvette. Typically, the six gases measured simultaneously by the MRGS set-up were SO<sub>2</sub>, NO<sub>2</sub>, CO, CO<sub>2</sub>, O<sub>3</sub>, and N<sub>2</sub>. The latter was used as an internal standard of the system, with the concentration of the N<sub>2</sub> gas in the ambient air being taken as the basis for normalization of results obtained from the other channels.

Manuscript received December 14, 1998; revised September 8, 1999. This work was supported in part by a project of the European Commission.

P. G. Papageorgas, D. Maroulis, and N. G. Theofanous are with the Department of Informatics, University of Athens, GR-15771 Athens, Greece.

H. Winter and H. Albrecht are with Laser-und Medizin-Technologie gGmbH, D-12207 Berlin, Germany.

Publisher Item Identifier S 0018-9456(99)09421-8.

block diagram for the RAMAN Multigas analyzer

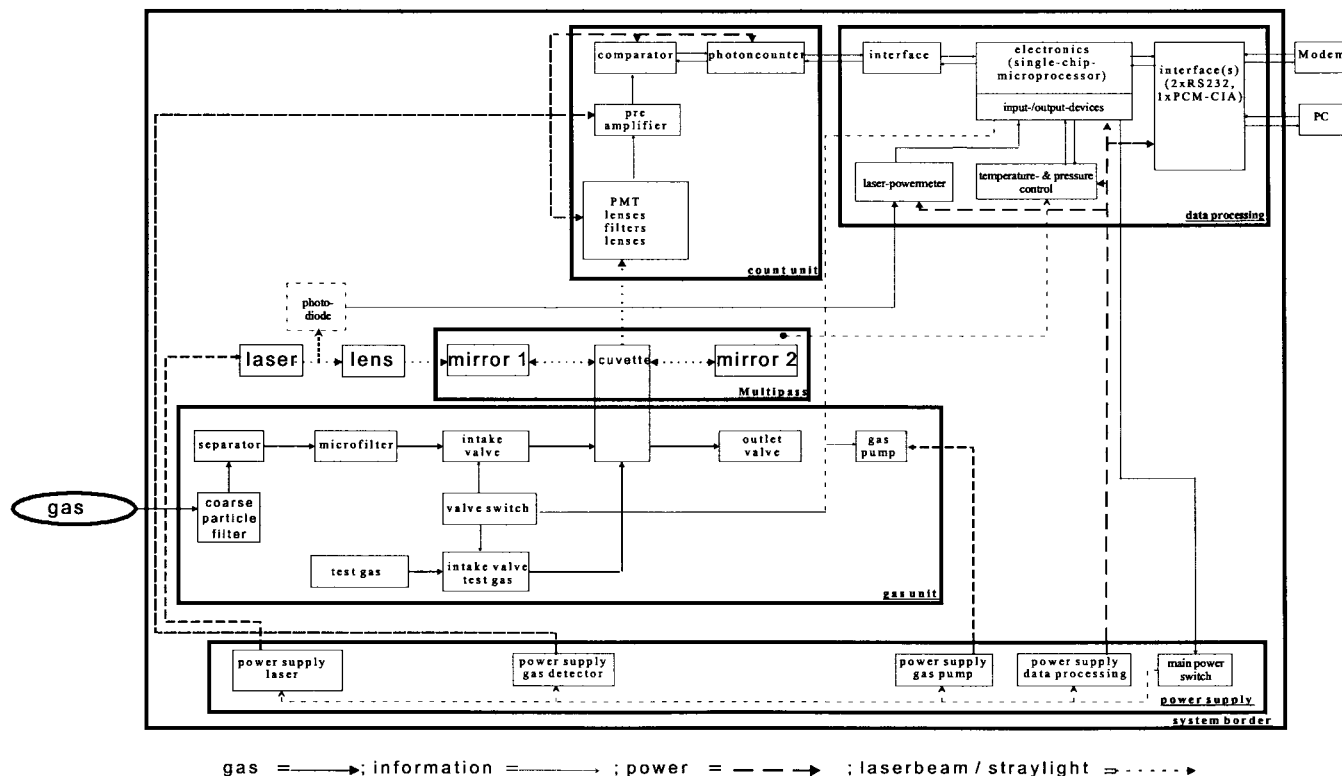


Fig. 1. Block diagram of the system.

The electric signals appearing at the outputs of the foregoing PMT's are collected by the six corresponding photon-counting modules/units of the multichannel photon-counting system. Each photon-counting module amplifies the corresponding PMT signal, discriminates it from the noise, and then after appropriate pulse shaping-the number of pulses is counted electronically. A digital microcontroller unit controls and coordinates the combined operation of the entire MRGS set-up. To that purpose, the microcontroller picks up the measurement outputs from all the photon-counting modules and performs an appropriate signal processing and storage of the so-collected data, while supporting an asynchronous communication line for the remote control of the system. Also, a practical gas sampling system is integrated in the set-up and, in addition, important variables such as temperature, pressure, relative humidity, and laser power are continuously measured, to make a conversion of the number of counts into concentrations (performed in the microcontroller unit of the system), on the basis of the equation of perfect gases. Finally, it is of note that, in the prototype implemented, the entire MRGS set-up has fit into a housing with dimensions  $60 \times 40 \times 40 \text{ cm}^3$  and the maximum electrical power consumption, for normal operation, was about 90 W.

### III. CONTROLLED MULTICHANNEL PHOTON-COUNTING SYSTEM

The controlled multichannel photon-counting (CMPC) system under presentation is composed of six similar photon-counting modules, each of which is inserted in the housing

of the corresponding PMT, and one microcontroller unit combined with appropriate sensors. Each photon-counting module consists of the following four circuit stages: The preamplifier stage, the upper level discriminator (ULD), the lower level discriminator (LLD), and the counter module. These stages, which in practice are realized by means of appropriate circuit boards, are depicted in the block diagram of the CMPC system shown in Fig. 2.

The preamplifier stage performs voltage amplification, from the voltage created by the photocurrent of the PMT at its  $50 \Omega$  resistance (to preserve the shape of one-photon-pulse the time constant of the PMT load should not exceed 5 ns, which implies a low PMT load resistance, typically  $50 \Omega$ ). The same stage is also intended to provide a matching of this resistance with the high input resistance of the subsequent discriminator stage. Hence, even if the output signal of the PMT is abundant, this preamplifier will be indispensable. The PMT used was the R3810P one manufactured from Hamamatsu Co. This specific PMT has a rise time of 0.6 ns, with one-photon amplitudes between 2–10 mV, and a gain in the order of  $10^7$ .

As to the role of the discriminators, it has to do with the fact that not all of the output pulses from each PMT are due to photons created from Raman scattering in the gas sample. Indeed, there are output pulses which are generated from internal noise in the load resistor and preamplifier circuit, from noise in the PMT itself (dark current, quantum noise of the incident light, Raleigh scattering, etc.) and from environmental radiation, cosmic rays included. As a result of that, the amplitude  $U$  of the useful pulses (i.e., of pulses due to photons

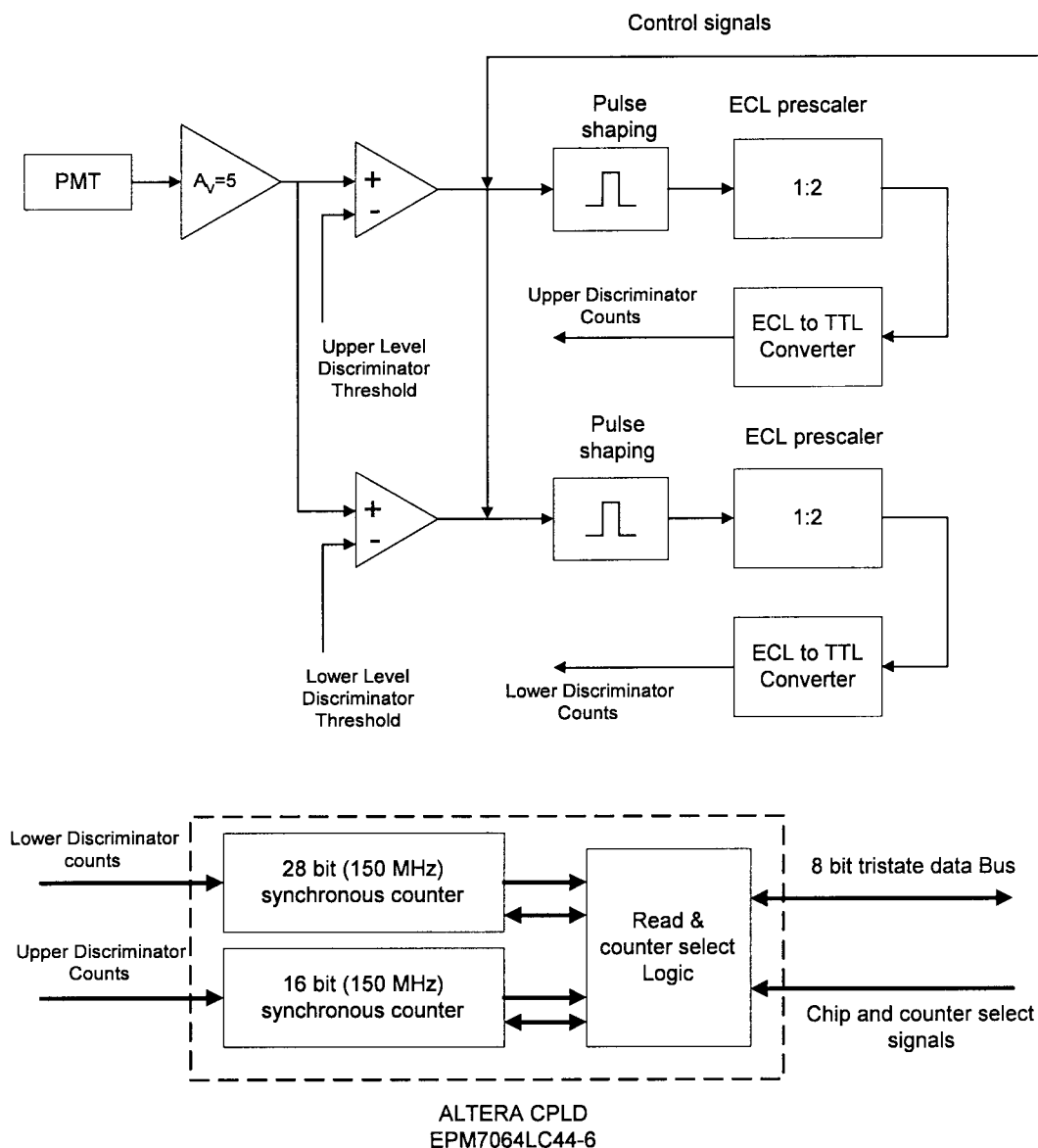


Fig. 2. Block diagram of the photon counting module.

from Raman scattering) should be discriminated from the amplitudes of pulses due to internal and PMT noise, (the PMT pulses are negative referenced to ground) that their absolute values are on the average noticeably smaller than a lower-level value  $U_{\min}$ , and the amplitudes of pulses due to environmental radiation, that their absolute values are on the average higher than an upper-level value  $U_{\max}$  [7], [9].

In accordance with the above, for cutting off the electronic noise contamination, a LLD has been introduced into the system, immediately after the preamplifier, and has been designed and adjusted so as to count all pulses with amplitude less than the lower-level threshold  $U_{\min}$ , which is empirically determined. Similarly, for removing the effect of electromagnetic radiation, particularly of cosmic rays, an ULD has been inserted in parallel with the LLD, as shown in Fig. 2, and has been arranged so as to count all pulses with amplitude less than the upper-level threshold  $U_{\max}$ , which is also empirically determined. Inversely, a gain control in the

preamplifier stage allows to amplify adequately the amplitude of the PMT output pulses in correspondence with given settings and thresholds of the LLD and ULD discriminators. The span between the above upper and lower thresholds of discriminators, i.e., the interval  $[U_{\min}, U_{\max}]$  will be referred to as the pulse window. In practice, this window is arranged by adjusting potentiometrically the reference voltages of the foregoing discriminators.

In our system, the detection of the Raman scattered light and the measurement of its optical intensity is made by counting the number of PMT output pulses, appearing in a given time interval, with amplitudes lying within the pulse window defined above. Consequently, after the LLD and ULD discriminators, a counter module is necessary for counting the digital pulses coming out from this pair of discriminators. This counter module has been implemented by means of a complex programmable logic device (CPLD). This CPLD device provides also a multidrop bus as it will be described below.

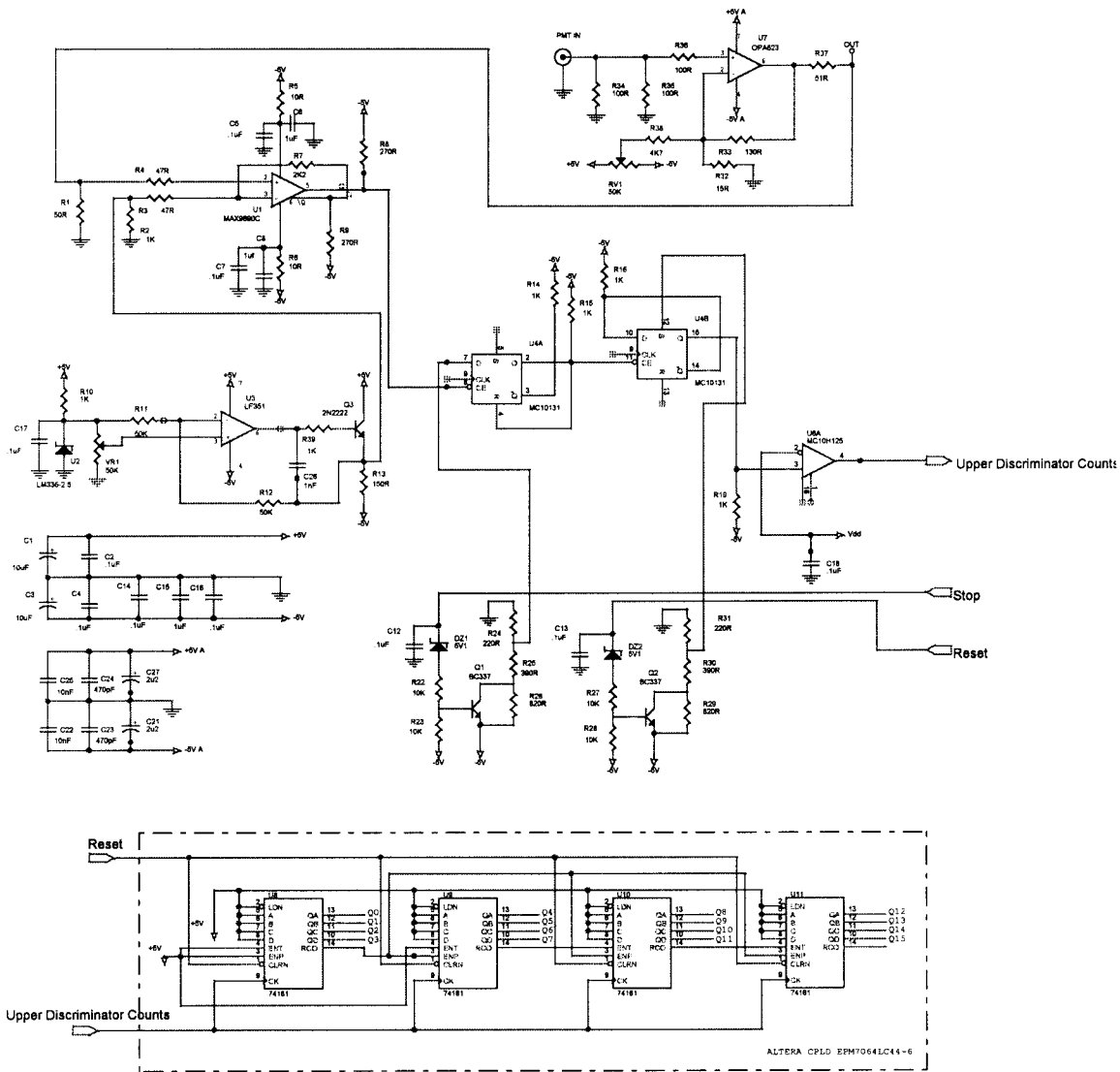


Fig. 3. Schematic diagram of the preamplifier, discriminator, and CPLD counter modules for the ULD.

The number of pulses with amplitudes within the specified pulse window is given from the difference between the counts measured by the above two counter circuits, over a given time interval, and is proportional to the individual concentration of the gas corresponding to the channel under consideration. In this type of measurements, the PMT's must be operating in the photon-counting mode. This mode has been judged indispensable not only because it fits very well the present photon-counting technique (which succeeds in rejecting most part of internal and environmental noise and therefore allows to measure weak light intensities) but also because it ensures increased dynamic range for the detected optical signals.

*A. Detailed Description of the Preamplifier and Discriminators Stages*

The preamplifier stage has been realized in the form of a small-size board on the basis of the Burr-Brown OPA623 operational amplifier, which has been found to be the best

solution as regards the cost and the power consumption of the chip. This chip is a current-feedback opamp with wide frequency bandwidth, excellent pulse-response slew rate (2100 V/ $\mu$ s) and very satisfactory rise time (1.9 ns). In the entire preamplifier stage, the amplification has been adjusted equal to 10, the bandwidth was nearly 200 MHz and the power consumption did not exceed 50 mW. In order to achieve high bandwidth without inciting ringing and oscillation effects, we have made use of very short board traces with sufficient ground planes, within the framework of a microstrip technique, and we employed resistors and capacitors of the SMD (surface mount device) type, which present low values of inductance. The LLD and ULD discriminators have been implemented as two identical boards. Each one of these boards consists of a high-bandwidth comparator, a pulse shaper, and a prescaler circuit. The schematic diagram of the so-realized discriminators is depicted in part of Fig. 3 (where only the ULD is shown).

In the practical system we have made use of the MAX960C comparator of Maxim Co., that exhibits a bandwidth of about

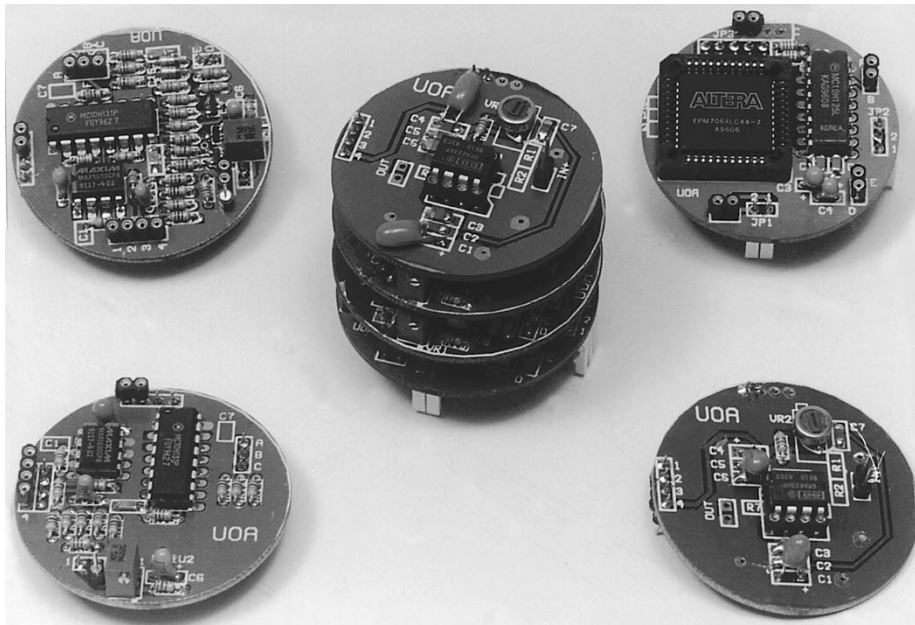


Fig. 4. Picture of the photon counting module. The A board is the preamplifier, B is the LLD, C is the ULD, and the D board contains the CPLD and the ECL/TTL converters.

600 MHz. The threshold level of the discriminators was arranged by adjusting, via the RV2 multiturn potentiometer/trimmer, the buffered voltage reference at the inverting input of the comparator (Fig. 3). This voltage reference is generated, with a value of 2.5 V, from the U2 chip in conjunction with the opamp U3, which acts as a buffer. The transistor Q3, connected in an emitter-follower configuration, provides an improved noise immunity and ensures a low impedance output that drives the inverting input of the comparator. Also, the comparator under consideration is operated in the Schmitt trigger configuration with positive feedback put on via the resistor R7. This arrangement provides an additional noise immunity that affords a useful positive hysteresis to the comparator [4]. In our case, this positive hysteresis has been set at 16 mV referenced to the input of the comparator. Hence, since in our system its input signal has been amplified by 5 (the gain of the preamplifier is 10 but this gain is divided by 2 due to the termination resistors at the output), an hysteresis of about 3.2 mV is created at the input of the system.

After the comparator, its output (being at ECL levels) is pulse shaped by the 1/2 U4 circuit, which is used as a monostable multivibrator. The output of this pulse shaper is a series of pulses with amplitudes at ECL levels and with constant time width of approximately 2 ns. The second half of the U4 chip provides a prescaling by 2 on the pulsed signal and is conveyed for counting to the counting module. The foregoing pulse shaper and prescaler stage has been implemented by means of the MC10H131 dual ECL flip-flop of Motorola Co. The common clock input (CLK), the set input (S) of the first flip-flop, and the reset input (R) of the second flip-flop are left open (LOW state). Also, the control of the counting channel is achieved by using the data input of the pulse shaping flip-flop. The required control signal is hardware generated from the memory chip of the microcontroller board, where a stabilizing crystal is used as a reference resulting in

high stability and precision for the counting period, which is software programmed in 5 ms steps. Also, the use of sockets for these chips has been avoided because of the significant parasitic inductance and capacitance that it can introduce.

On the other hand, the transistors Q1 and Q2 have been used, in conjunction with the DZ1 and DZ2 zener diodes, to provide translation of the two reset and start/stop control signals from TTL to ECL levels. As to the U10 and U11 chips, they are voltage regulators for the power supplies of the various integrated circuits of the implemented board.

One of the most important aims considered during the design of the photon-counting system was the reduction of the noise that can be coupled to the system (from electric and/or magnetic fields) and could interfere with the measurements. The circuit layout and shielding are playing a critical role in the performance of the system. The ground of the low voltage, high-bandwidth, signals at the preamplifier section is made separate from the ground of the digital sections and a star topology was followed for the common ground [11], [12]. Special attention has been given to the grounding points of the different sections with a view to avoiding ground loop effects that can deteriorate the system performance. We must also mention that we have used separate voltage regulators for the power supply of each prescaler in order to cope with the interference between these adjacent units due to the large currents floating, during counting, at the power supply of the digital section. We have used also separate isolated high-voltage power supplies for each PMT, avoiding in this way any interference between the different channels due to ground loops.

### B. Counter Module

The counter module, implemented by means of six counter boards (one for each PMT output), includes the level translation circuits and a CPLD device, which realizes the individual

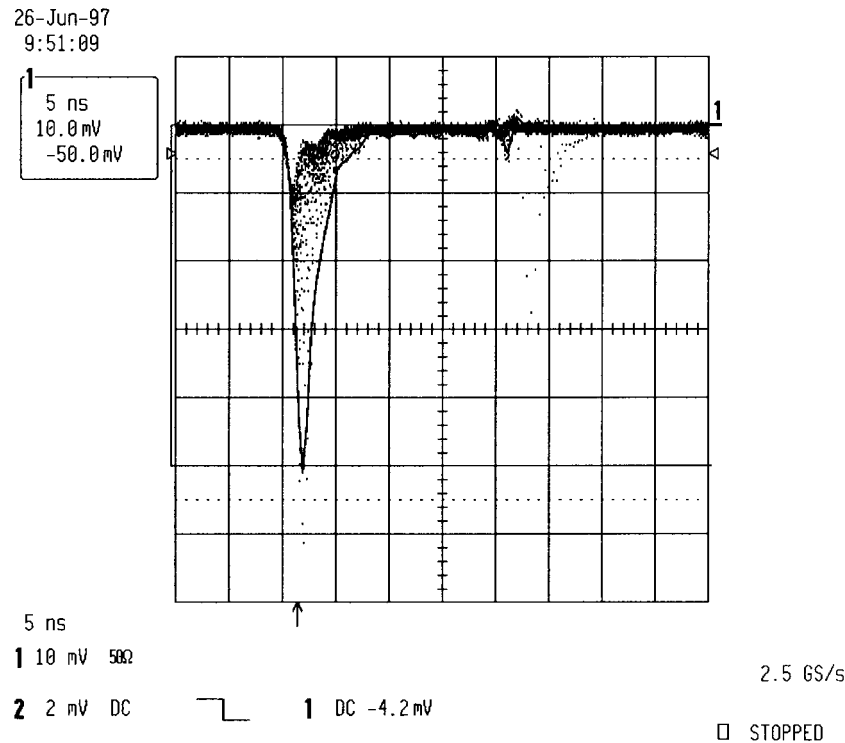


Fig. 5. Oscilloscope measurement at the preamplifier input.

counters and also supports a multidrop byte-wide bus for the interface affected with the microcontroller board. Each of the six so-supported counter boards is identified by a specific address and the communication with the microcontroller takes place in a serial access sequence, during which the microcontroller interrogates successively—one after another—all of the counter boards.

The ECL outputs from the two discriminators are level translated to TTL logic via a MC10H125 IC of Motorola Co. and then the so-resulting pulse train is directed for counting to the CPLD device. The second input of each ECL/TTL translator is connected to the internally produced bias voltage ( $V_{dd}$ ) in order to use the translator in the single ended mode of operation. In our system, this device was an EPM7064LC44-6 chip of Altera Co. that is implemented using the EEPROM-based  $0.6 \mu\text{m}$  CMOS technology.

The CPLD device under consideration provides two synchronous counters, which are used for counting the pulses after the upper and lower level discrimination, respectively. Typically, the ULD counter has a width of 16-bits while the LLD counter has a width of 28-bits. These widths have been found adequate for the present Raman gas sensor, in which the Raman scattering effect gives scattered light having low to medium intensity levels. Anyway, to obtain a CMPC system usable also for other applications demanding higher count widths (e.g., for counting higher light levels), we have supplemented the present unit with an overflow detection circuit using the interrupt mechanism of the systems microcontroller. The latency of an interrupt event with the microcontroller used in practice was less than  $50 \mu\text{s}$  and this value is effectively adequate for most photon-counting applications. In our system, with its own interrupt mechanism and an appropriate software

we have realized counters with a total width of 32-bits.

One part of the schematic diagram of the as above CPLD-based counter is presented in Fig. 3 for the ULD counter. In this unit, the concept of count-enable trickle/count-enable parallel design, which was pioneered via the popular 74 161 TTL-MSI counter, has been used for the realization of a fast nonloadable synchronous binary counter of arbitrary width. In this manner, prescaler-counter designs originate with small, high-speed counters such as the prescaler described in the previous paragraph. These counters are used to divide an incoming clock frequency and, thereby, provide a new clock to a larger, slower counter. Note also that the carry look-ahead circuitry of the 74 161 provides for cascading counters in case of applications demanding N-bit synchronous stages without additional gating. In the system, the terminal count of the least significant 74 161 was used as a parallel clock enable for the other remaining counters. This scheme has effectively reduced the clock rate for these counters by a factor of 16, thus allowing their ripple-enable path 16 times longer to settle. The corresponding maximum clock frequency allowed a maximum counting frequency of 150 MHz and, with the ECL prescaler (having a factor of two), this frequency mounted up to approximately 300 MHz. Hence, as the preamplifier used has a bandwidth of approximately 200 MHz, this is the maximum counting frequency imposed on the entire CMPC photon-counting system. This maximum frequency is adequate for most, even demanding, photon-counting applications encountered in practice, as it gives a pulse pair time resolution of approximately 5 ns.

In Fig. 4, we have a photo of the photon-counting module with the boards comprised that are stacked one over the other. The preamplifier is at the A board, while the LLD is at the B

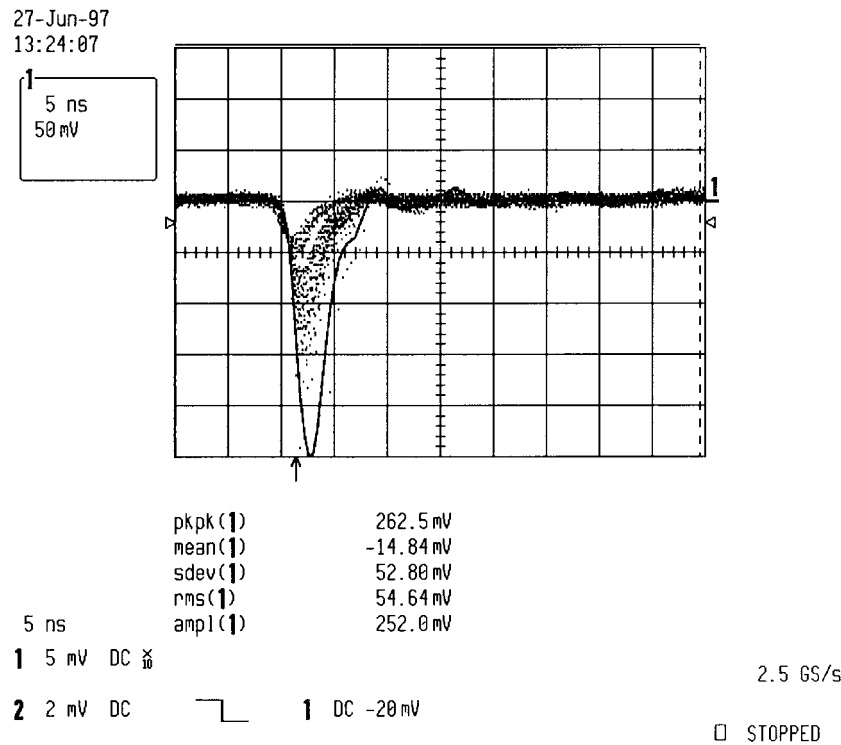


Fig. 6. Oscilloscope measurement at the comparator input.

board, in C board we have the ULD, and the D board contains the CPLD together with the ECL to TTL converter. In this photo we can also see an assembled photon-counting module, which has overall dimensions of 4 cm diameter and 5 cm height.

### C. Microcontroller Unit

An 87C196KC microcontroller of Intel Co. constitutes the basis of a single board microcomputer which supports the data acquisition and control functions in the present MRGS. This microcontroller unit is combined with an NVRAM (nonvolatile RAM) memory, which is the type of memory that we have adopted in the design of the control unit for the storage of software and data because it meets the need for software upgrade that is becoming increasingly important in embedded systems. Note that the above microcontroller includes 16 kB of OTP (one time programmable) ROM on chip. A small software library is stored into this memory, which supports mainly an asynchronous RS-232C communication with a host computer and a command parser for the remote control of the unit.

Upon initial power-up, the 87C196 will be initialized by the bootstrap program that is loaded in the OTP ROM: then the execution of the main program follows and the control is transferred to the code area of the NVRAM. Subsequent uploads of software upgrades can be performed once the system is in the field using the RS-232 interface.

The data acquired from the counter module are stored in the NVRAM of the control unit. The serial communication of this system with a host computer based on a portable PC allows the mass storage of data along with further processing and versatile presentation of the acquired data. In this portable

PC a user interface has been developed, for the communication with the embedded system, using the Labwindows CVI development software from National Instruments Co.

The 87C196KC microcontroller under consideration has, as a core, a 16-bit CPU and, besides the 16 kB of OTP ROM, includes two programmable 16-bit timers/counters, a full duplex serial I/O port with dedicated Baud rate generators, prioritized interrupt sources, 40 I/O pins, 8 channel/10-bit A/D converter with sample/hold, and it has a power consumption of 10 mA working at 20 MHz clock frequency derived from a crystal oscillator.

On the other hand, the NVRAM memory has been implemented with the DS1386-32 chip of Dallas Semiconductors. This chip comprises (in one package) a static RAM of 32 kB, a real-time clock, and a watchdog programmable timer, along with a lithium battery and all the circuitry that is needed for the operation of the real-time clock and the retention of data in the RAM memory for at least ten years. The watchdog operation serves to reset the whole system in case the programmed time slice would happen to expire without a normal canceling of the watch-dog operation from the main program, which means that a software fault exists. It is of note that the entire data area in the NVRAM memory is separated into two sections; the first 4 kB are used for the application program and the remaining 28 kB are used for the storage of the acquired data. This memory capacity is sufficient for the storage of the average 15-min values of all the six channels throughout the time period of one week.

Finally, the software for the entire control system supports the concurrent execution of three tasks. The corresponding

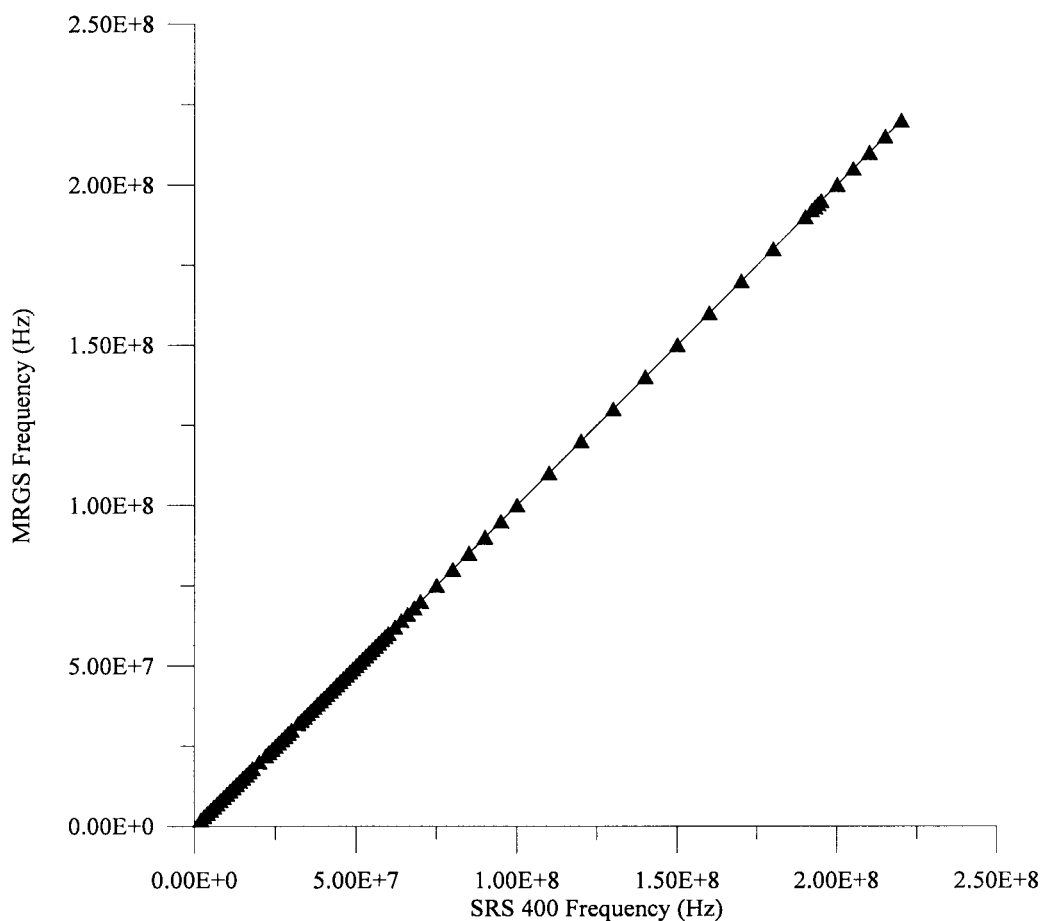


Fig. 7. Comparison of frequency measurement between the MRGS and the SRS400.

multitasking implementation was not round-robin but preemptive event driven with an appropriate interrupt mechanism. The above three tasks can be described as

- 1) collection of data;
- 2) preprocessing and storage of collected data;
- 3) remote control asynchronous communication.

#### D. Sensors and Actuator Control

For the correct operation of the entire MRGS system, a number of physical quantities must be measured by appropriate accessories of the microcontroller unit and must be stored in the microprocessor unit along with the values of concentrations measured by the system for the monitored gases or pollutants. These quantities or parameters measured in our prototype are

- 1) absolute temperature at two important points (i.e., in ambient air and inside the cuvette);
- 2) absolute pressure (in the ambient air);
- 3) differential pressure (between the ambient air and inside the cuvette);
- 4) relative humidity of air;
- 5) optical power of the laser beam.

Knowledge of the values of these quantities/parameters is necessary for the translation of the photon counts measured for each gas into concentration values.

To measure temperature outside and inside the cuvette, we used the DS1620 digital thermometer manufactured by Dallas

Semiconductors Co. This chip measures temperature in the range of  $-55\text{ }^{\circ}\text{C}$  to  $+125\text{ }^{\circ}\text{C}$  with a resolution of  $0.1\text{ }^{\circ}\text{C}$  and accuracy of  $0.5\text{ }^{\circ}\text{C}$ . The output of this chip is a 9-bit word obtained, in a serial form, every 1 s. The as above two values from temperature measurements are collected from the microcontroller unit using four digital ports.

For the measurement of the absolute pressure and the differential pressure we used the 142SC15A and 142SC01D pressure sensors, respectively, of Sensym Co. These sensors, which measure pressures up to 15 and 1 psi, respectively, include in the same chip circuitry for temperature compensation and signal conditioning and provide a voltage output that is directly digitized by the 10 bit A/D of the microcontroller.

The relative humidity was measured inside the cuvette, with a Humicap sensor, which is a capacitive-type humidity sensor manufactured by Vaisala Co. This sensor has very small dimensions and therefore its placement inside the cuvette is fairly easy. The sensor is operating as a capacitive element of an oscillating circuit and in this manner the humidity is converted to oscillator frequency, which is measured by one of the high speed digital inputs of the microcontroller unit.

As to the light intensity of the laser beam, it is monitored with a precision of 1% via a light-to-frequency converter, precisely the TSL220 one manufactured by Texas Instruments Co. The frequency at the output of this converter is measured with one of the four high-speed digital inputs of the microcontroller unit.

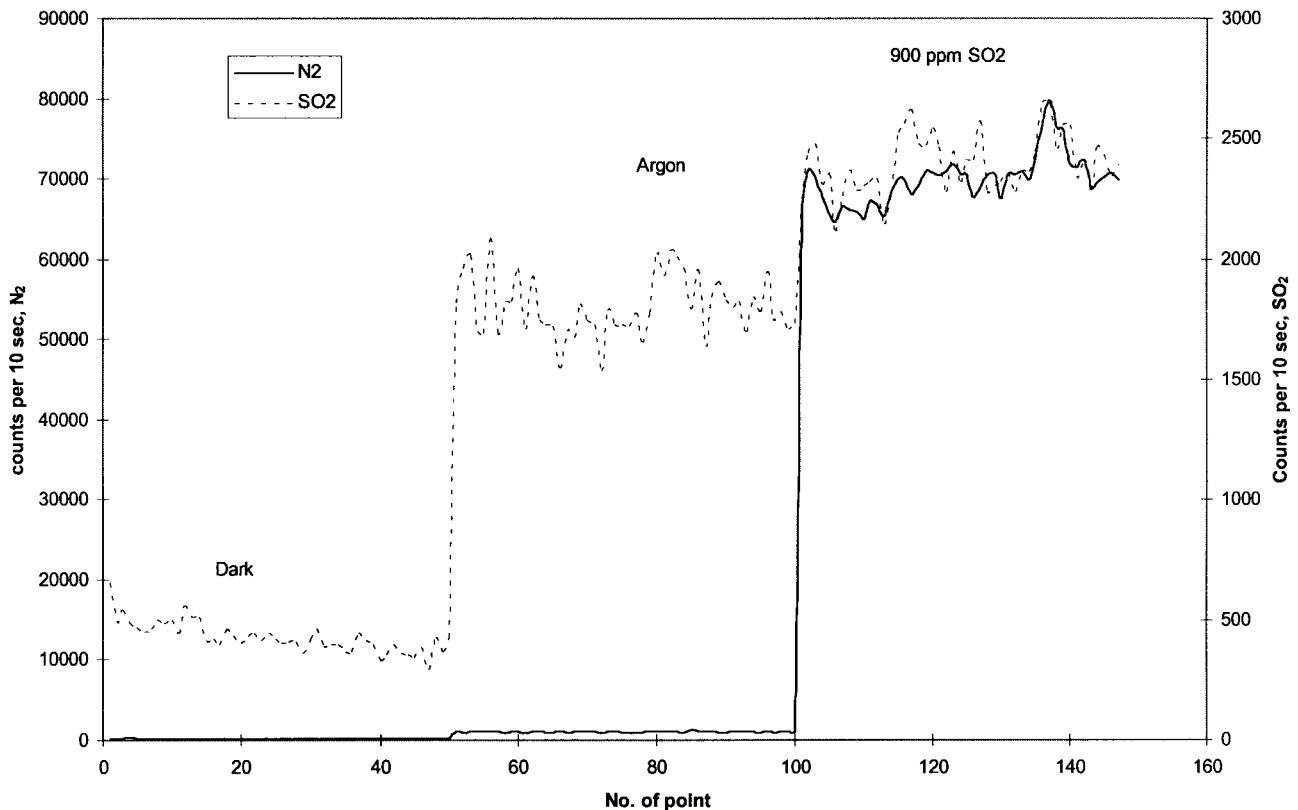


Fig. 8. Experiment for measurement of the sensitivity for  $\text{SO}_2$ .

The cuvette is provided with a gas sampling system which comprises the following parts:

- 1) three valves (inlet, outlet and calibration valve) for the flow control of the gas sample or the calibration gas;
- 2) a pump for the suction of the gas sample;
- 3) an electromechanical shutter, electronically controlled, for the monitoring of the laser source.

All the above various types of actuators are controlled via seven digital outputs of the microcontroller, which are optoisolated from the circuits of actuators in order to achieve reduction of the interference noise due to relatively the high currents flowing through them. For the same reason, isolated dc/dc converters are used for the power supply of the actuators board.

#### IV. PERFORMANCE MEASUREMENTS

A number of experiments have been conducted in order to define the performance of the developed photon-counting system. First of all, we have made extensive tests regarding the noise level at the analog parts of the discriminator sections, because these are the most important points for the proper operation of the photon-counting system.

Figs. 5 and 6 show the shape of the PMT pulses at the input of the preamplifier and at the input of the comparator, respectively. From Fig. 6 the rise and fall times were measured and found equal to 3.8 and 1.6 ns, respectively. In the

extraction of the final results, the internal resistance and capacitance of the oscilloscope probe have been taken into account. The digital oscilloscope used was the LeCroy 9361 type with 300 MHz bandwidth and a sampling rate of 2.5 Gsamples/s. An averaging of 20 s was selected in order to reveal the characteristic features of the PMT signals. From the above figures we can see that two important requirements of the system are fulfilled.

- 1) Noise of the system at the comparator input is around 2 mV peak-to-peak.
- 2) Full-width-at-half-maximum (FWHM) value, which can be taken as a measure of the time resolution, is around 3 ns.

Tests were conducted using signal generators up to 200 MHz and a commercial photon-counting unit (SR400 type from Stanford Research Systems Co.) as reference. These experiments were performed using identical discriminator level settings. Fig. 7 shows measurement results obtained for comparison between the described system and the SRS400 system. As signal source, a DS345-type synthesized function generator was used for frequencies up to 30 MHz. For higher frequencies, up to 220 MHz, the Schomandle SG1000 RF generator was used.

To examine the reliability and accuracy of the count measurements made by our MRGS system, two basic parameters were adopted, respectively, the bias and precision defined as

TABLE I  
ANALYSIS FOR THE DETERMINATION OF SO<sub>2</sub> SENSITIVITY

<b>Argon floating through gas cell</b>		
		<b>SO2 Norm. to N2 (counts/10-sec)</b>
<i>mean value</i>	$X_{\text{mean}}$	19.53
<b>sqrt mean value</b>	$\text{SQRT}(X_{\text{mean}})$	4.42
<b>standard deviation</b>	s	1.97
<b>mean error1 (68%)</b>	$s/\text{SQRT}(n)$	0.28
<b>rel. error (68%)</b>	$s/\text{SQRT}(n)/X_{\text{mean}}$	1.4%
<b>900 ppm SO<sub>2</sub> in 3.8 N<sub>2</sub> floating through gas cell</b>		
		<b>SO2 Norm. to N2 (counts/10-sec)</b>
<i>mean value</i>	$X_{\text{mean}}$	2110.00
<b>sqrt mean value</b>	$\text{SQRT}(X_{\text{mean}})$	45.93
<b>standard deviation</b>	s	181.03
<b>mean error2 (68%)</b>	$s/\text{SQRT}(n)$	25.60
<b>rel. error (68%)</b>	$s/\text{SQRT}(n)/X_{\text{mean}}$	1.2%
<b>usable Signal</b>		2090.47
<b>mean error (68%)</b>	$\text{SQRT}[(\text{mean err. 1})^2 + (\text{mean err. 2})^2]$	25.60
<b>rel. error (68%)</b>		1.22%
<b>concentration [ppm]</b>		900
<b>sensitivity [ppm]</b>	<b>usable Signal &gt; mean error</b>	11.02
<b>sensitivity [ppm]</b>	<b>usable Signal &gt; 2* mean error</b>	24.25

follows:

$$\text{bias} = \frac{1}{N} \sum_{i=1}^N (\text{MR}_i - \text{SR}_i)$$

$$\text{precision} = \left[ \frac{1}{N} \sum_{i=1}^N (\text{MR}_i - \text{bias} - \text{SR}_i)^2 \right]^{1/2}$$

where  $\text{MR}_i$  is the MRGS measurement result,  $\text{SR}_i$  is the SRS400 measurement result, and  $N$  is the number of observations. The bias was measured equal to  $-7$  counts, while the precision was estimated to be 10 counts. For the frequency range covered (1–220 MHz), these results correspond to an error between the MRGS and the SRS400 less than 1 ppm, which is quite acceptable considering that most commercially available photon counters have a precision of about 10 ppm.

Note that the main source of error for absolute counting measurements is the crystal oscillator, that is used for the determination of the counting time interval, along with the electronics used for translation from TTL to ECL. Due to the ratiometric nature of our system (because of the fact that the measurement for each channel is normalized with respect to the measurement obtained from the  $N_2$  channel) it was not necessary to develop a high accuracy oscillator circuit or to use special electronics for the generation of the control signal of the counting time interval.

A conclusion deduced from the measurements performed as above is that our photon-counting system can detect pulses with amplitudes  $\geq 2$  mV referenced at the input and can

TABLE II  
SENSITIVITIES FOR THE MEASUREMENT OF CONCENTRATIONS WITH GREEN AND BLUE LASER

<b>Gas</b>	<b>Green Laser Sensitivity</b>	<b>Blue Laser Sensitivity</b>
<b>N<sub>2</sub></b>	< 0.5 %	< 0.5 %
<b>SO<sub>2</sub></b>	< 50 ppm	< 100 ppb
<b>CO<sub>2</sub></b>	< 15 ppm	60 ppb
<b>NO<sub>2</sub></b>	< 0.5 ppm	60 ppb
<b>O<sub>3</sub></b>	not determined	not determined
<b>C<sub>6</sub>H<sub>6</sub></b>	< 50 ppm	< 0.50 ppm
<b>CO</b>	300 ppm	< 0.50 ppm

count with a pulse-pair resolution better than 5 ns with a bandwidth of 200 MHz. For comparison, we point out that the SRS400 system has a pulse-pair resolution of 5 ns, a bandwidth of 300 MHz, can detect pulses with a minimum amplitude of 2 mV and has an accuracy of  $2 \text{ ns} \pm 1\%$  in the determination of the count interval. Therefore, we can state

that, to some degree, our system lacks the analog bandwidth and accuracy in the time interval definition that the SRS400 system has, but has comparable sensitivity limits. On the other hand, for applications of the present type, the accuracy in the above time interval is not crucial. By contrast, issues such as the realization of a multiple photon-counting system and the portability asset, in which our system offers certain advantages, are more important.

#### V. INDICATIVE MEASUREMENTS ON TEST GASES

To evaluate our photon-counting system as part of the entire MRGS setup, we have realized with it a complete setup and taken a set of measurements of concentrations for various gases involved in air pollution. In this context, we present the results of determination of sensitivity in the case of measuring the SO<sub>2</sub> concentration. In Fig. 8, we illustrate the time series of such an experimentation, in which the measurement procedure follows the steps below:

- 1) determination of dark-count-rates;
- 2) base-line test with non-Raman active gas (Argon);
- 3) test gas.

The test gas is SO<sub>2</sub>, with a concentration of 900 ppm, mixed with N<sub>2</sub> having purity 99.98%. The Argon was used as a base-line (background) test gas because, as monatomic gas, does not produce Raman scattering. The difference in the counting results between the Argon and the SO<sub>2</sub> measurements gives the usable signal from which the mean error of the measurement by the system under test is estimated. The total mean error is calculated as the result of contributions of two independent noise sources, that is, the sum of the mean error during the SO<sub>2</sub> measurements and the mean error during the Argon measurements. The usable signal is divided by the mean error multiplied by 2, in order to check that we have a S/N-ratio  $\geq 2$ . The photon-counting system developed was used in the sensitivity determination experiments with a 10-s integration time and the discriminator setting was  $-4$  mV referenced at the input of the signal. Each measurement step consists of approximately 50 independent 10-s measurements. Table I shows the analysis results after normalization as to the N<sub>2</sub>-channel. This normalization has been accomplished by taking the peak value of the N<sub>2</sub>-channel during the whole measurement period and dividing each 10-s measurement of the N<sub>2</sub>-channel with this value and then multiplying with the corresponding 10-s measurement of the SO<sub>2</sub> channel. In this way, errors due to fluctuations in the laser power are minimized. The sensitivity achieved was found equal to approximately 24 ppm.

It is of note that the use of a blue excitation laser (457 nm) instead of the green one would improve significantly the sensitivity of the entire system. This can be seen from the experimental results listed in Table II, which have been obtained by using the optical part of the entire MRGS system combined with the SRS400 unit of Stanford Co. Indeed, as it can be seen from a recent article [3], the proposed system has superior performance and, moreover, it can measure simultaneously five different gases. The normalization procedure referred to

the nitrogen concentration of the ambient air affords to our system the self-calibration and drift compensation features that are very important for the prolonged operation of such a system without operator assistance.

#### VI. CONCLUSIONS

Apart from its simplicity, low power consumption, portability, and low cost, the photon-counting system described in this work presents a number of advantages:

- 1) preamplifier-discriminator stages exhibit a bandwidth of 200 MHz;
- 2) good thermal stability in the amplifier and discriminator sections;
- 3) satisfactory low noise level (less than  $400 \mu\text{V}_{\text{p-p}}$  referenced to the input of the system).

The described photon-counting system represent an economical exploitation of multichannel Raman scattering effect targeting to commercial applications. Compared to a system based to a single channel Raman scattering the present one offers satisfactory insensitivity to variations in excitation intensity and to changes in sample properties or errors in the optics, thus resulting in stable quantitative measurements. The cost of the introduced photon-counting system per channel is clearly less than any existing commercial solution having similar performance. Of course this opens opportunities for low-cost development of laboratory setups using PMT's for multichannel applications.

#### REFERENCES

- [1] A. Weber, P. S. Porto, L. E. Cheesman, and J. J. Barrett, "High-resolution Raman spectroscopy of gases with CW-laser excitation," *J. Opt. Soc. Amer.*, vol. 57, pp. 19–28, 1967.
- [2] H. Albrecht, G. Müller, and M. Schaldach, "Application of laser Raman spectroscopy to medical diagnosis II," in *Proc. 6th Int. Conf. Raman Spectroscopy*, Bangalore, India, Sept. 4–9, 1978, vol. 2, pp. 526–527.
- [3] P. C. Kumar and J. A. Wehrmeyer, "Stack gas pollutant detection using laser Raman spectroscopy," *Appl. Spectrosc.*, vol. 51, no. 6, pp. 849–855, 1997.
- [4] N. R. Malik, *Electronic Circuits—Analysis, Simulation, and Design*. Englewood Cliffs, NJ: Prentice-Hall, 1995, ch. 2 pp. 119–122.
- [5] A. Weber, *Raman Spectroscopy of Gases and Liquids, Topics in Current Physics*. Berlin, Germany: Springer-Verlag, 1979.
- [6] V. S. Lebedev and V. D. Lysov, "A photon-counting circuit," *Instrum. Exper. Tech.*, vol. 18, no. 6, pp. 1776–1777, 1975.
- [7] Y. E. Tiberg and V. N. Paulauskas, "One-electron pulse selector circuit for photon counting systems," *Instrum. Exper. Tech.*, vol. 23, no. 5, pp. 1252–1255, 1980.
- [8] A. M. Evtushenkov, Y. F. Kiyachenko, G. I. Olefirenko, and I. K. Yudin, "Photon-counting system for correlation amplitude measurements," *Instrum. Exper. Tech.*, vol. 24, no. 5, pp. 1265–1267, 1981.
- [9] K. D. Shelevoi, "High-speed differential pulse discriminator-counter," *Instrum. Exper. Tech.*, vol. 28, no. 3, pp. 614–616, 1985.
- [10] S. A. Zakamaldin and L. V. Victorov, "Instrument for study of single-electron photomultipliers," *Instrum. Exper. Tech.*, vol. 28, no. 3, pp. 614–616, 1989.
- [11] R. Morrison, *Grounding and Shielding Techniques in Instrumentation*. New York: Wiley, 1986.
- [12] H. W. Ott, *Noise Reduction Techniques in Electronic Systems*. New York: Wiley, 1988.

**Panagiotis G. Papageorgas** was born in Euboia, Greece, in 1961. He received the B.Sc. degree in physics and the Ph.D. degree in applied physics from the University of Athens, Greece, in 1984 and 1995, respectively.

From 1985 to 1991, he was a Teaching Assistant with a doctoral fellowship in the laboratories of Electronics and Meteorology, Department of Applied Physics, University of Athens. His dissertation research was on the development of sound detection and ranging systems. Since 1988, he has been teaching digital electronics as a Professor in the Military School of Telecommunications and Electronics. Since 1994, he has been with the Department of Informatics, Division of Communications and Signal Processing, as a Researcher in European projects in the development of electronic instrumentation for air-pollution and biomedical applications.

**Harald Winter** was born in Oberhausen, Germany, in 1962. He received the B.Sc. degree in physics from the Free University of Berlin, Germany, in 1992. He is currently pursuing the Ph.D. degree.

From 1988 to 1992, he was a Tutor in geology, medicine, and pharmacy. From 1993 to 1999, he was a Freelance Scientist at the Institute for Laser-und Medizin-Technologie, Berlin.

**Hansjörg Albrecht** was born in Stuttgart, Germany, in 1942. He received the B.Sc. degree in physics from Stuttgart and Hamburg Universities in 1969 and the Ph.D. degree in 1976.

From 1969 to 1971, he was a Development Engineer with AEG-Telefunken, Berlin, Germany, and from 1971 to 1978, he was a Scientist with the Central Institute for Biomedical Engineering, Erlangen-Nuremberg University. From 1978 to 1983, he was a Scientist with DFVLR and from 1984 to 1989, he was Head of Product Management Monitoring with Dräger AG, Lübeck, Germany. From 1989 to 1990, he was a Scientific Adviser and Head of Physicochemical Technologies Department with the Laser-Medizin-Zentrum, Berlin. Since 1990, he has been the Managing Director of LMZ Berlin, reorganized in 1995 into LMTB.

**Dimitris Maroulis** was born in Naxos, Greece, in 1949. He received the B.Sc. degree in physics, the M.S. degree in radioelectricity, the M.Sc. degree in electronic automation, and the Ph.D. degree in physics, all from the University of Athens, Greece, in 1973, 1977, 1980, and 1990, respectively.

In 1979, he was appointed Assistant and, since 1991, he has been Lecturer and Assistant Professor in the Department of Informatics, University of Athens. He is currently teaching and performing research activities, including projects with the European Community. His main areas of activity include signal processing, real-time systems, and optoelectronics with applications in digital communications and biomedical systems.

**Nikiforos G. Theofanous** was born in Ioannina, Greece, in 1940. He received the B.Sc. degree in physics, the M.S. degree in radioelectricity, the Ph.D. degree in physics, and the M.Sc. degree in electronic automation, all from the University of Athens, Greece, in 1964, 1971, 1973, and 1975, respectively.

In 1969, he was appointed Assistant and in 1973, Chief Assistant in the Electronics Laboratory, University of Athens, for the period up to 1981. In 1982, he was elected Lecturer and in 1984, Assistant Professor, in the Department of Physics, University of Athens. In 1990, he was transferred to the Department of Informatics of the same university, where, in 1991, he was elected Associate Professor, and in 1995, Full Professor in electronics and optoelectronics. He is currently working in the above department in teaching and research activities, including projects with the European Community. His main areas of activity include electrooptics, fiber optics, and optoelectronics with applications in optical communications and in optoelectronics biomedical systems.

Dr. Theofanous is President of the Greek Laser and Electrooptics Scientific Society.